Some Thermodynamic and Kinetic Properties of the System PETG-CO_2, and Morphological Characteristics of the CO_2-Blown PETG Foams*

Y. PAUL HANDA,† BETTY WONG, *and* ZHIYI ZHANG

Institute for Chemical Process and Environmental Technology
National Research Council
Ottawa, Ontario, Canada K1A 0R6

VIPIN KUMAR *and* SHARON EDDY

Department of Mechanical Engineering
University of Washington
Seattle, Washington 98195

KISHAN KHEMANI

Eastman Chemical Company
Kingsport, Tennessee 37662

Reprinted from POLYMER ENGINEERING AND SCIENCE, January 1999, Vol. 39, No. 1

Some Thermodynamic and Kinetic Properties of the System PETG-CO_2, and Morphological Characteristics of the CO_2-Blown PETG Foams*

Y. PAUL HANDA,† BETTY WONG, *and* ZHIYI ZHANG

Institute for Chemical Process and Environmental Technology
National Research Council
Ottawa, Ontario, Canada K1A 0R6

VIPIN KUMAR *and* SHARON EDDY

Department of Mechanical Engineering
University of Washington
Seattle, Washington 98195

KISHAN KHEMANI

Eastman Chemical Company
Kingsport, Tennessee 37662

The solubility of CO_2 in PETG, a glycol-modified PET, was measured at different temperatures and over a broad pressure range, and diffusion coefficients were derived at the corresponding conditions. The solubility of CO_2 is quite high. For example, almost 15 wt% CO_2 can be dissolved in PETG at 35°C and 6.0 MPa. Consequently, CO_2 is a good blowing agent for PETG. Cellular foams in the density range of about 0.04 to 1.2 g/cm^3 and cell diameters in the range of about 10 to 150 μm were produced. The foam density and the cell size were found to depend on the foaming temperature and time, with larger cells obtained at higher temperatures or when the sample was foamed for a longer time. The foam density decreased with an increase in the foaming temperature to about 90°C, beyond which the density tended to increase slightly due to the cell collapse or coalescence. The density reduction also depended on the pressure at which the polymer was saturated with CO_2; the higher the saturating pressure at a given temperature, the greater the density reduction.

INTRODUCTION

Polymer foams having closed cells of size 10 μm or smaller and a cell density of about 10^8 cells cm^{-3} or higher are called microcellular foams. Such morphologies can be produced by the phase inversion of a polymer solution via a temperature quench or with a liquid antisolvent (1), by polymerization in a near-critical fluid followed by supercritical drying (2), or by injecting the polymer solution into an antisolvent vapor or supercritical fluid, usually CO_2 (3–5). However, for polymers with low glass transition temperatures, T_gs, microcellular foams have most often been produced from CO_2-saturated polymer solutions. Consequently, there is a growing interest in developing CO_2-based processes for making polymer foams. The use of CO_2 as a blowing agent offers many advantages — it is easily available, it has a relatively low critical temperature, its equation of state is accurately known, and it is soluble to a considerable extent in solid polymers. The latter allows CO_2 to easily plasticize the polymer matrix, thus making it the blowing agent of choice in producing microcellular foams. The solubility of CO_2 in polymer melts remains appreciably high to allow the

*Issues as NRCC No. 41978.
†To whom correspondence should be addressed; paul.handa@nrc.ca

production of foams with larger cells. Thus, a whole range of foams can be made using the same blowing agent.

The use of CO_2 in producing microcellular morphology in several polymers with relatively low T_gs has been well established by now (6). The procedure normally used is to contact the polymer with high-pressure CO_2 to obtain a saturated solution. The system is then subjected to a sudden thermodynamic instability by either rapidly raising its temperature to slightly above the polymer's nominal T_g (7, 8) or by releasing the gas pressure at a temperature above the plasticized T_g (9). In either case, CO_2 escaping from the polymer matrix nucleates a large number of small, closed cells whose morphology is quenched when the system temperature falls below its T_g or the system is depleted of CO_2.

PETG is an amorphous, glycol-modified poly(ethylene terephthalate) made from terephthalic acid, ethylene glycol, and cyclohexanedimethanol by a polycondensation process. However, unlike PET, it does not undergo crystallization on heating or on plasticization by the dissolved species; the comonomer, cyclohexanedimethanol, is responsible for the completely amorphous nature of this polymer. PETG has a low T_g and a high melt strength, and it has been successfully evaluated for producing medium density foamed sheets by extrusion using CO_2-evolving chemical blowing agents (10). Previous studies (11, 12) have shown that PETG has high a affinity for CO_2, and is easily processed into foams with varying cell sizes. In this paper we report further investigations on the foamability of PETG using CO_2 as the blowing agent.

EXPERIMENTAL

The PETG used was Eastman's Eastar 6763 copolyester in the form of extruded films and was supplied by Eastman Chemical Company. Some characteristics of the polymer used were: $\overline{M}_n$ = 26 000, T_g = 77°C, and density = 1.29 g/cm^3. High purity CO_2 (SFE grade) was obtained from Air Products.

Gas solubilities were obtained using two different gravimetric techniques. In one of the techniques, hereby called the continuous method, a Cahn D110 microbalance was used to conduct sorption and desorption studies on CO_2 in PETG at 35°C and pressures to about 7 MPa. The details of the technique are decribed elsewhere (13). Briefly, about 1 g of polymer, in the form of 12 mm diameter × 0.25 mm thick disks, was placed on the sample side of the balance, and glass beads weighing approximately the same as the PETG sample were installed on the reference side. An appropriate amount of nichrome wire was then added to the sample side such that the mass and volume of the two sides were as matched as possible in order to minimize the effect of buoyancy.

The sample was degassed for three days at 35°C before starting the measurements. At a given pressure, the microbalance simply recorded mass every 10 s until a constant value was obtained. Once the system attained constant mass, the pressure was increased to the next value, and this was continued until the final pressure was about 7 MPa. Then the pressure was decreased in small steps, establishing constant mass at each step. The measurements were continued until the final pressure was about zero. The experimental data were corrected for shifts in the balance zero as a function of pressure, and for buoyancy due to the small volume difference between the sample and reference sides that developed as the polymer dilated due to dissolution of the gas.

The other gravimetric technique used was the batch method, and it has been described previously (11). Measurements were made at 26.7, 40, 50, and 60°C and at pressures to 6 MPa. The sorption and desorption runs were conducted by placing a known amount of the polymer sample in a high pressure vessel and then pressurizing or depressurizing the system with CO_2. The vessel was opened periodically to weigh the sample. This was continued until a constant mass was obtained. With this technique, some loss of the dissolved gas during the handling and weighing procedures is inevitable. This loss of gas depends primarily on the diffusion coefficient of the gas, and on the surface-to-volume ratio of the polymer sample—the smaller the ratio, the smaller the gas loss. But this reduction in mass loss comes at the expense of increased equilibration time. Consequently, measurements were made with PETG films of thicknesses 0.25, 0.51, 0.76, and 1.0 mm in order to provide a cross-check on the equilibrium solubilities and the sorption/desorption kinetics.

The plasticization effect of CO_2 was examined by measuring the change in T_g of the PETG-CO_2 system as a function of the gas pressure (or gas solubility). A high pressure DSC (Setaram DSC121) modified for scanning samples while in contact with a high pressure gas was used. The details of the technique have been described elsewhere (14). About 50 mg PETG film with a thickness of 0.76 mm was loaded into the DSC sample vessel and degassed for an hour prior to being exposed to compressed CO_2 at 35°C and a given pressure for three hours. The T_gs of the saturated samples were determined by scanning the samples from 15°C to 100°C at a rate of 5°C/min under the same CO_2 pressures as those used during saturation. The midpoint of the step transition was taken as the glass transition temperature.

For producing foam samples, PETG films of size 30 mm × 10 mm × 0.76 mm were saturated with CO_2 at room temperature for three hours in a pressure vessel. The pressure was then gradually released and the saturated films were quickly placed in a preheated oven for a specified time to foam the sample. The foamed specimens were quenched in tap water to freeze the morphology. The effect of the variables such as foaming temperature, foaming time, and the saturating pressure on the foam properties was investigated. The densities of the foamed PETG samples were

tion is obtained on foaming for longer times at lower temperatures than at higher temperatures.

At lower foaming temperatures, the density of the foam is close to that of the unfoamed PETG. As the foaming temperature is increased, the density decreases rapidly before leveling off at a temperature near 90°C, *Fig. 4*. During the foaming process, the gas continually diffuses out of the PETG matrix causing the T_g of the system to increase. When the T_g surpasses the foaming temperature, the cell growth stops. At higher temperatures, the diffusion of CO_2 into the cells is more rapid and the polymer molecules are more mobile. As a result, the cell size increases thus giving foams with lower densities. However, cells can easily coalesce or collapse at foaming temperatures above the polymer's T_g, resulting in increase in the density as seen in *Fig. 5* and also observed previously in other polymers (22). The shape of the cells also depends on the foaming temperature as shown in *Fig. 7*. Small, spherical cells are formed at lower temperatures. As the foaming temperature is raised, the size of the cells increases and their shapes become influenced by the neighboring cells, and as they continue to expand, they acquire polyhedral structures.

ACKNOWLEDGMENT

The authors thank Mr. Gerry Pleizier for assistance with the SEM work.

REFERENCES

1. A. T. Young, *J. Cellular Plastics*, **23**, 55 (1987).
2. G. Srinivasan and J. R. Elliot, *Ind. Eng. Chem. Res.*, **31**, 1414 (1992).
3. A. K. Lele and A. D. Shine, *AIChE J.*, **38**, 742 (1992).
4. D. J. Dixon and K. P. Johnston, *J. Appl. Polym. Sci.*, **50**, 1929 (1993).
5. D. J. Dixon, G. Luna-Bárcenas, and K. P. Johnston, *Polymer*, **35**, 3998 (1994).
6. V. Kumar, *Cellular Polymers*, **12**, 207 (1993).
7. J. E. Martini, F. A. Waldman, and N. P. Suh, *SPE ANTEC Tech. Papers*, **28**, 674 (1982).
8. J. E. Martini-Vvedensky, N. P. Suh, and F. A. Waldman, U.S. Patent 4,473,665 (1984).
9. S. K. Goel and E. J. Beckman, *Polym. Eng. Sci.*, **34**, 1137 (1994)
10. Anonymous Research Disclosure, Derwent WPI, 1994, CC No. RD362028.
11. V. Kumar, S. Eddy, and R. Murray, *SPE ANTEC Tech. Papers*, **42**, 1920 (1996).
12. Y.-T. Shieh, J.-H. Su, G. Manivannan, P. H. C. Lee, S. P. Sawan, and W. D. Spall, *J. Appl. Polym. Sci.*, **59**, 707 (1996).
13. B. Wong, Z. Zhang, and Y. P. Handa, *J. Polym. Sci.: Part B: Polym. Phys.*, **36**, 2025 (1998).
14. Z. Zhang and Y. P. Handa, *J. Polym. Sci.: Part B: Polym. Phys.*, **36**, 977 (1998).
15. D. S. Pope, G. K. Fleming, and W. J. Koros, *Macromolecules*, **23**, 2988 (1990).
16. C. M. Balik, *Macromolecules*, **29**, 3025 (1996).
17. R. M. Felder, *J. Memb. Sci.*, **3**, 15 (1978).
18. Y. P. Handa, S. Lampron, and M. L. O'Neill, *J. Polym. Sci.: Part B: Polym. Phys.*, **32**, 2549 (1994).
19. M. L. O'Neill and Y. P. Handa, *Assignment of the Glass Transition, ASTM STP 1249*, R. J. Seyler, editor, American Society for Testing and Materials, Philadelphia, 1994.
20. T. S. Chow, *Macromolecules*, **13**, 362 (1980).
21. V. Kumar and J. Weller, *J. Eng. Ind.*, **116**, 413 (1994).
22. V. Kumar, J. E. Weller, and R. Montecillo, *J. Vinyl Technol.*, **14**, 191 (1992).

rated polymer is scanned in a conventional DSC because of the outgassing process, which interferes with the calorimetric signal. The T_gs thus obtained either have a large uncertainty or may not even represent the actual thermal event for the polymer-gas system. As seen in *Fig. 3*, our results show a linear decrease in T_g with increasing pressure (or concentration). This trend is similar to that observed in other polymer-CO_2 systems (14, 18, 19) and is in agreement with Chow's model (20). When extrapolated to 3.6 MPa, our results in *Fig. 3* give a T_g of about 45°C, in reasonable agreement with the results in *Fig. 2*.

The density of PETG foams as a function of foaming temperature is shown *Fig. 4*. The corresponding cell sizes and cell densities are plotted in *Figs. 5* and *6*, respectively. Here, the cell density is expressed as the number of cells per gram of the polymer and was obtained by dividing the number of cells per unit volume of foam by the foam density. The advantage of this method is that no assumptions on the cell structure are required for the calculations. Also shown in *Fig. 6* are the cell densities calculated from the foam density and cell size results in *Figs. 4* and *5*, respectively, assuming that cell size and number determine the void space in the foam. Since the SEM measurements usually underestimate the cell size, the calculated results are slightly higher than the ones based on SEM measurements; otherwise the trend shown by the two sets of results is the same. The maximum in cell density observed at 60°C in *Fig. 6* is similar to that found in CO_2-blown polycarbonate foams at a temperature well below the T_g of the neat polymer (21). The reason for a maximum in cell density is that both nucleation and cell growth rates increase with foaming temeprature and both phenomena compete for the gas available in the system. This leads to a *trade-off* at some optimum temperature where a maximum in cell density is observed.

Microcellular foams are characterized by cell sizes around 10μm. For the results shown in *Figs. 4–6*, the foam samples were produced by saturating PETG with CO_2 at room temperature and 5.6 MPa. Under these conditions, the T_g of the system is already depressed to room temperature as suggested by the results in *Fig. 3*. Consequently, as seen in *Fig. 5*, microcellular structures are obtained at foaming temperatures in the range 40–60°C. In general, it was found that the higher the saturating pressure, the lower the temperature at which a given density reduction could be obtained. For example, a density reduction of 50% was obtained at 50°C when PETG was saturated with 4.8 MPa CO_2, and at 90°C when it was saturated with 1.4 MPa CO_2. The results shown in *Figs. 4–6* are for samples foamed for 120 s. As reported previously (11), the foam density also depends on foaming time—the density decreased as the foaming time was increased, and the extent of density reduction depended on the foaming temperature. Thus, at saturating conditions of 26.7°C and 4.8MPa, the density decrease with respect to unfoamed PETG was 5% after 10 s and 20% after

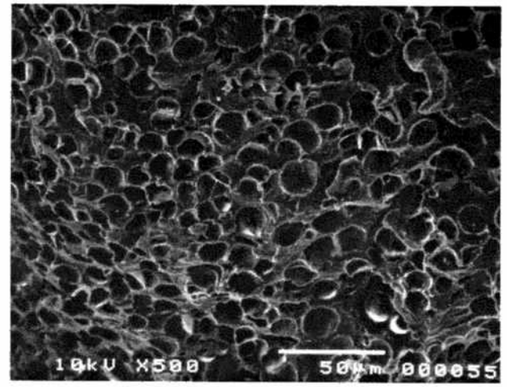

Fig. 7. SEM photographs of the CO_2-blown PETG foams showing details of the cell morphologies. Foaming temperature: top photograph, 60°C; middle photograph, 80°C; bottom photograph, 140°C.

120 s at a foaming temperature of 40°C, and was 80% after 10 s and 90% after 120 s at the foaming temperature of 80°C. Thus, a relatively larger density reduc-

determined by weighing in water and in air using a balance with a resolution of 10 μg. For microstructural analysis, the foamed samples were fractured at liquid nitrogen temperature. The freshly exposed surface was sputter coated with a thin layer of gold and then micrographic pictures were taken using a scanning electron microscope (JEOL, JSM-5300). The photographs were scanned into the computer, phase inverted, and printed using a high resolution printer. The cells in the phase-inverted photographs were colored manually, and then rescanned into the computer for image analysis using Image Pro Plus software from Media Cybernetics. During the image analysis, the background of each scanned photograph was adjusted so that only the colored cells were visible on the computer screen. All the statistics such as equivalent diameter, perimeter, and area, and their distributions in each sample were obtained from the analysis.

RESULTS AND DISCUSSION

The sorption and desorption solubilities C obtained by the continuous and the batch methods are shown plotted against pressure p in *Fig. 1*. Solubilities obtained by the batch method are usually lower than the equilibrium values (13) because of the loss of dissolved gas during the handling and weighing procedures, and this is seen to be the case here also. As seen in *Fig. 1* for the results at 35°C, the dual-mode behavior is not as prominent during the sorption run as it is during the desorption run. At pressures higher than about 2.0 MPa, the sorption and desorption solubilities are about the same. At lower pressures, sorption/desorption hysteresis can be seen and the desorption solubilities are higher owing to the irreversible dilation of the polymer matrix during the sorption run. Such hysteresis effect has been observed for most solid polymers (13, 15). The C-p plots for the sol-

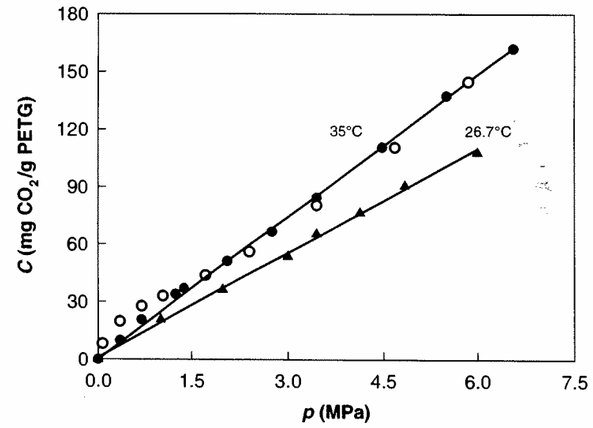

Fig. 1. Solubility of CO_2 in PETG plotted against the gas pressure. Values at 26.7°C were obtained by weghing the gas-saturated samples under ambient conditions, and those at 35°C were obtained using a high-pressure microbalance. ● - sorption and ○ - desorption runs at 35°C.

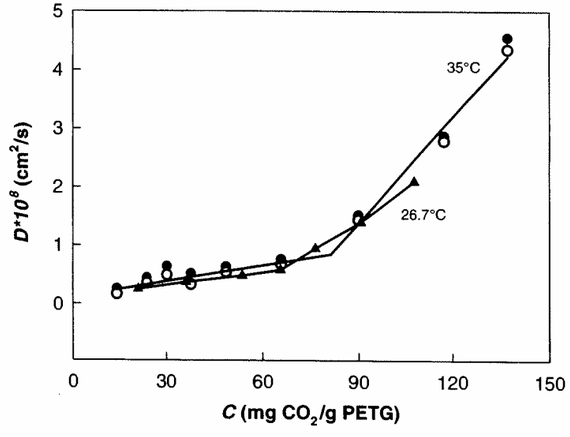

Fig. 2. Diffusion coefficients of CO_2 in PETG. ● - values obtained from the sorption kinetic data at 35°C and using the hybrid function of Eqs 1 and 2, ○ - values obtained from the sorption kinetic data at 35°C and using Eq 4, Δ - values obtained from the desorption kinetic data at 26.7°C and using the truncated form of Eq 1.

ubilities obtained at 40, 50, and 60°C by the batch method were linear, similar to the plot shown at 26.7°C in *Fig. 1*. The solubility coefficients, defined as C/p, obtained from these results are 20.1, 17.2, 14.0, and 12.0 (mg CO_2/g PETG) MPa^{-1} at 26.7, 40, 50, and 60°C, respectively. This gives a temperature coefficient of –0.25 (mg CO_2/g PETG) MPa^{-1} K^{-1} for the solubility coeffcient, and can be used to extrapolate the solubility results at 35°C obtained with the microbalance over a limited temperature range.

For thin, flat film geometry, the kinetics of sorption (desorption) at short and long times are given by *Eqs 1* and *2*, respectively

$$\frac{M_t}{M_\infty} = \frac{4}{h}\left(\frac{Dt}{\pi}\right)^{\frac{1}{2}} + \frac{8}{h}(Dt)^{\frac{1}{2}}\sum_{n=1}^{\infty}(-1)^n \, ierfc\left(\frac{nh}{2(Dt)^{\frac{1}{2}}}\right) \quad (1)$$

$$\frac{M_t}{M_\infty} = 1 - \frac{8}{\pi^2}\sum_{n=0}^{\infty}\frac{1}{(2n+1)^2}\exp\left(\frac{-(2n+1)^2\pi^2 Dt}{h^2}\right) \quad (2)$$

where M_t and M_∞ are the mass uptake (or loss) at time t and $t = \infty$, respectively, h is the film thickness, and D is the diffusion coefficient. Normally, either *Eq 1* or *2* truncated after the first term in the expansion is used to obtain D. However, the hybrid method proposed recently (16) combines the equations for gas transport kinetics at short and long times into a single function, and has been shown to be superior to using the truncated from of *Eq 1* or *2*. The sorption kinetics can also be reduced to a moment defined as (17)

$$\tau = \int_0^\infty \left(1 - \frac{M_t}{M_\infty}\right) dt \quad (3)$$

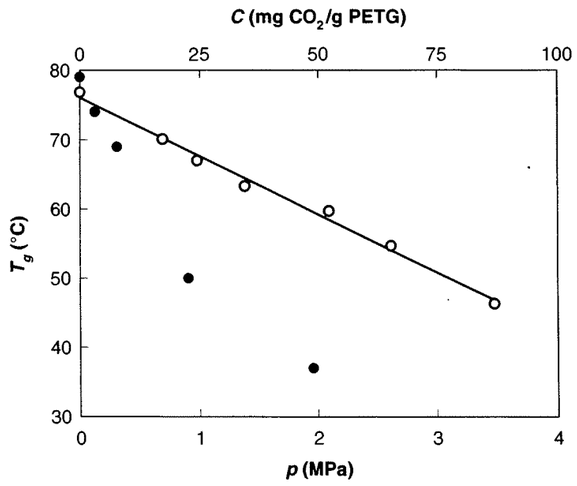

Fig. 3. T_g of PETG-CO_2 system plotted against the pressure at which the polymer was saturated (bottom axis) and the corresponding equilibrium solubility (top axis). ○ - our results obtained with the high-pressure DSC, ● - literature values (12) obtained using a conventional, ambient pressure DSC. A line is drawn through our results to show the trend.

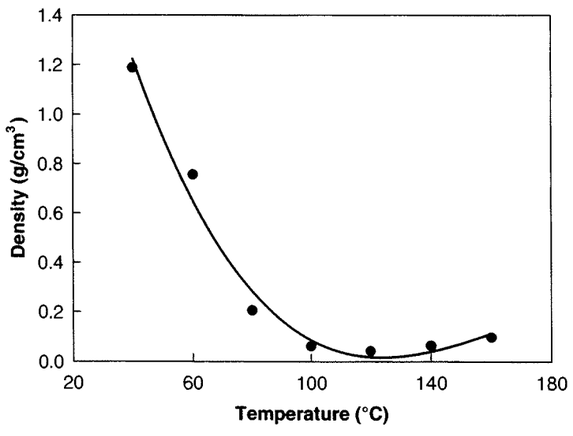

Fig. 4. Density of CO_2-blown PETG foam plotted against foaming temperature. A curve is drawn through the data points to show the trend.

which can then be related to the diffusion coefficient by

$$D = \frac{h^2}{12\tau} \quad (4)$$

A detailed description of the data analyses in terms of *Eqs 1–4* has been described elsewhere (13). The diffusion coefficients calculated from the microbalance results at 35°C using the hybrid and the moment methods are in excellent agreement, as seen in *Fig. 2*. The diffusion coefficients increase with increasing solubility because of the plasticizing effect of CO_2. At about 8 wt% loading, corresponding to a pressure of about 3.6 MPa, there is a change in the concentration dependence of D. A similar inflection is also observed in the desorption solubilities at 35°C shown in *Fig. 1*. At this concentration of dissolved CO_2, the polymer undergoes transition from the glassy state to the rubbery state. Also shown in *Fig. 2* are the diffusion coefficients obtained from the desorption kinetics data obtained at 26.7°C by the batch method, and using the first term on the right hand side of *Eq 1*. The two gravimetric techniques produce the same qualitative trend, though there is some disagreement between the two sets of diffusion coefficients, and the onset of the glass→rubber transition is predicted to be at different temperatures.

T_g values for the system PETG-CO_2 as determined by high pressure DSC are shown plotted against pressure (and the corresponding equilibrium solubility at 35°C) in *Fig. 3*. Also shown in *Fig. 3* are the literature results (12) obtained by scanning the CO_2-saturated PETG samples in a DSC under ambient pressure. The literature values suggest a much sharper decrease in T_g than observed in the present work. However, as reported previously (14, 18), the assignment of a glass transition is somewhat ambiguous when a gas satu-

Fig. 5. Cell diameter of the foamed samples plotted against foaming temperature. A curve is drawn through the data points to show the trend.

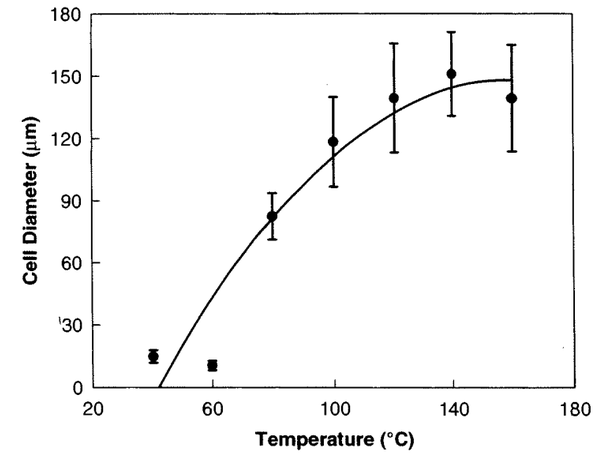

Fig. 6. Cell density of the foamed samples plotted against foaming temperature. A curve is drawn through the data points to show the trend. ● - measured values, ○ - calculated from the data in Figs. 4 and 5.